J Mater Sci (2010) 45:6424–6432
DOI 10.1007/s10853-010-4727-6

Investigation of structural and optical properties of the CdS and CdS/PPy nanowires

Nurdan D. Sankir · Bahadir Dogan

Received: 22 October 2009 / Accepted: 17 June 2010 / Published online: 2 July 2010

Abstract In this study, cadmium sulfide (CdS), polypyrrole (PPy) nanowires, and their heterojunctions have been electrochemically synthesized. Morphology of the nanowires has been investigated by scanning electron microscopy. Energy dispersed X-ray, X-ray diffraction, UV–Vis, and FTIR analyses have been used to confirm structure of both CdS and PPy nanowires. For the first time with this study, CdS/PPy nanowire heterojunctions have been integrated into photoelectrochemical (PEC) cells. It has been also demonstrated that PEC performance of the nanowires was strongly function of production conditions, such as deposition time and voltage. The maximum power conversion efficiency of the CdS nanowires obtained in this study was 1.36%. Moreover, efficiencies of the CdS/PPy nanowires have been reached to 5.00%, which makes them very favorable for PEC applications.

Introduction

Cadmium sulfide (CdS) thin films are the most promising candidates for photoelectrochemical (PEC) applications due to its high optical absorption, ease of manufacturing techniques, and proper band-edge positions for maintaining reduction/oxidation of water [1, 2]. Although, there are many studies about CdS thin films, there is very limited information about CdS nanowires integrated into PEC cells [3, 4]. Among these limited studies, Jang et al. [4] have been reported the solvothermal synthesis of CdS nanowires with 3.0 mA/cm^2 photocurrent density and 6 μmol/h hydrogen evolution rate in 0.1 M Na_2S + 0.02 M Na_2SO_3 electrolyte solution. Similarly, Dongre et al. [3] have been reported the improvement of the junction ideality factor by replacing the CdS nanoparticles with nanowires in PEC cell. On the other hand, organic–inorganic hybrid (OIH) heterostructures have been gaining more attention, since they combine the high performance of inorganic materials with lower production cost and easy manufacturing techniques of organic materials [5, 6]. OIH thin films have been used to fabricate electric and optoelectric devices for more than a decade with the improvement in both material science and device architectures. For example, inorganic nanowires such as germanium [7], silicon [8], zinc oxide [9], and cadmium selenide [10] have been utilized in organic semiconductor thin films for photovoltaic applications. However, one can easily notice that the major drawback of such architecture in these studies is low charge carrier mobilities of organic semiconductor thin films. On the other hand, nanowires from organic semiconductors can offer a rapid transport path for charge carriers due to their one-dimensional nature [11–13]. Therefore, hetereojunction structure from organic and inorganic semiconductor nanowires could be crucial. To our knowledge, there has been no report in the literature on the CdS/organic hybrid hetero-nano structures for PEC applications. We report herein the simple and cost effective electrochemical fabrication of the CdS and polypyrrole (PPy) nanowires to demonstrate their PEC performances. Also, morphological, structural, optical, and photoelectrochemical properties of CdS/PPy nanowires have been investigated in this study.

Experimental

CdS nanowire deposition was performed using gold-coated anodized alumina membranes (AAM, Whatman Anodisc

N. D. Sankir (✉) · B. Dogan
Nanotechnology and Membrane Science Laboratory, TOBB University of Economics and Technology, Ankara, Turkey
e-mail: nsankir@etu.edu.tr

47) immersed into a solution containing 055 M $CdCl_2$ (Aldrich) and 0.19 M elemental sulfur (Aldrich). Solution temperature was kept at 125 °C. In order to investigate the effects of processing conditions on nanowire formation, two different deposition voltages and times have been chosen. Figure 1 shows schematic illustration of the experimental setup used for CdS nanowire formation. After CdS nanowire deposition, PPy (Pyrrole from Aldrich) nanowires synthesis on the same electrode by using 0.1 M $LiClO_4$, 0.01 M pyrole, and 7×10^{-4} M sodium dodecyl sulfate took place. During synthesis, potential was swept between 0 and 0.85 V at a scan rate of 400 mV/s for various numbers of CV scans (Fig. 2). Morphological characterization of the thin films has been performed using a QUANTA 400F Field Emission Scanning Electron Microscope. In order to perform scanning electron microscopy (SEM), energy dispersed X-ray (EDX), UV–Vis, and FTIR measurements, templates were dissolved in 1 M NaOH solution after coating one side with epoxy resin. The absorbance spectra of the samples were measured by a Pharmicia LKB Ultraspec III UV–VIS spectrophotometer over the wavelength range of 325–900 nm at room temperature. In order to confirm the crystal structure of the films, α Rigaku Miniflex X-ray diffraction (XRD) system equipped with Cu Kα radiation has been used. PEC cell configuration has been formed with CdS or CdS/PPy nanowires as working electrode into a three-electrode configuration in one compartment cell, with a graphite counter electrode and Ag/AgCl reference electrode. Electrical response of the nanowires under illumination (35 mW/cm^2) has been recorded using a Gamry G750 Potentiostat/Galvanostat/ZRA system, where 0.1 M Na_2S, 0.1 M NaOH, and 0.1 M S solution were used as electrolyte.

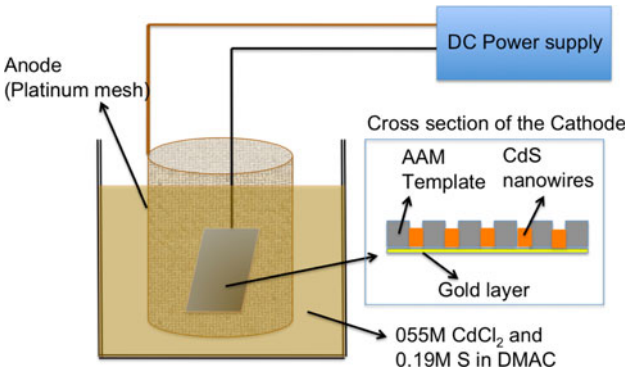

Fig. 1 Schematic illustration of electrodeposition of CdS nanowires

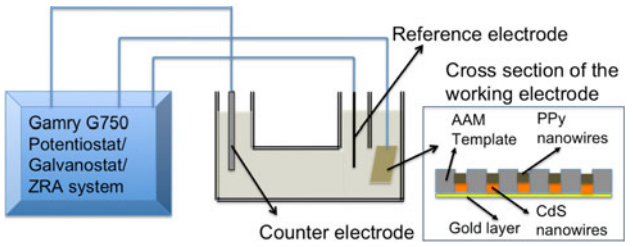

Fig. 2 Schematic illustration of electrodeposition of CdS/PPy nanowires

Results and discussion

Formation of CdS and CdS/PPy nanowires

Bias voltage, deposition temperature, and time are the key factors affecting the CdS nanowire formation. It has been observed that solubility of the elemental sulfur is very poor for the temperature lower than 100 °C. Therefore, no CdS nanowire formation has been observed for temperatures lower than 100 °C. This result is consistent with previously reported CdS nanowire studies [14]. For temperatures higher than 130 °C, the gold layer evaporated on the AAM was damaged. Hence, the electrochemical CdS nanowire formation failed at temperatures higher than 130 °C. This problem can easily be overcome by increasing the thickness of the gold layer by further material deposition. For practical reasons we preferred controlling the temperature of the system rather than varying the thickness of the metal layer of the substrate. The temperatures ranging between 100 and 125 °C have been found as the optimum temperature range for CdS nanowire formation. Typically, in an electrochemical nanowire formation charged reactive species in the solution diffuse through the pores of the template and reach the electrode surface by means of an applied electric field. Similarly, electrochemical formation of CdS nanowire can be considered in two steps. When an electric field is applied, Cd^{2+} ions enter to the pores of the template. At cathode, reduction of Cd^{2+} ion occurs and Cd^0 reacts with S^0, which enters into the pores by the diffusion process, to form CdS. Nucleation and growth process of CdS nanowire occurs in the pores of the template. Hence, the pore size, density, and wetability affect the morphology of nanowire. In this study, AAM is used as template due to its high thermal and chemical stability. The average pore size of the AMM used here was 0.02 μm. SEM analysis has been performed to investigate the CdS nanowire formation and effect of the process conditions on morphology. As can be seen in Fig. 3a, b, CdS nanowires deposited for 10 min are much shorter than the nanowires deposited for 30 min. It has also been observed that diameter of the CdS nanowires deposited for 10 min is smaller than the nanowires deposited for 30 min. The diameter of the nanowires produced at 10 min was about 100 nm. On the other hand, the diameter and the length of the nanowires produced at

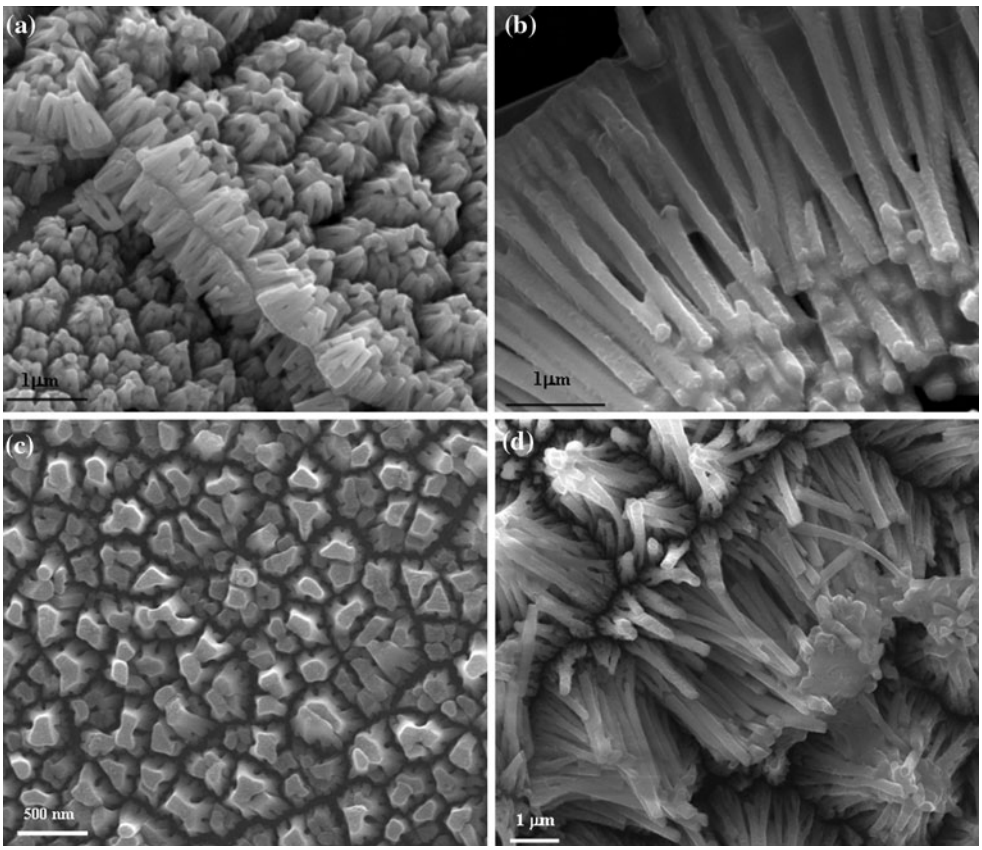

Fig. 3 SEM images of CdS nanowires grown at **a** 125 °C, 30 V for 10 min, **b** 125 °C, 30 V for 30 min, **c** 125 °C, 20 V, 30 min, **d** 100 °C, 30 V, 30 min

30 min reached about 200 nm and 4 μm, respectively. This can possibly attributed to the fact that nucleation of the CdS nanowires starts on the bottom of the AAM pore instead of the pore wall. Then nanowire formation may occur on top of this seed layer in both upward and sideward dimensions. A significant change in morphology, where CdS nanowires turned into very small in length and in diameter, has been observed for the nanowires deposited at the same temperature and time, but at lower voltages (i.e., 20 V) (Fig. 3c). This could be attributed to insufficient applied electric field for the nucleation of CdS nanowires. Therefore, a few separate CdS seeds formed at the bottom and they coalesced whenever a critical material deposition was obtained. In addition, there has been no significant difference in morphology for the nanowires deposited at 100 °C (Fig. 3d).

Reynes and Demoustier-Champagnez [15] have been reported that either PPy nanotube or nanowire formation occurs depending on the pore size of the template, pyrrole monomer concentration, and CV scan rate. Herein, the length and the diameter of the PPy nanowire have been controlled by the number of CV scans. Figure 4a, b shows the SEM images of these PPy nanowires deposited in gold-coated AAM. It has been observed that when the number of CV scan increased at constant scan rate, both the length and the diameter of the PPy nanowires increased. The average length and the diameter of the PPy nanowires formed after 200 scans were about 3 μm and 300 nm, respectively. When the number of scan increased to 800, average length and the diameter of the nanowires reached to 26 μm and 400 nm, respectively. In all cases the surface of the PPy nanowires was rough and so indicating the random nucleation position. This could be attributed to the absence of molecular anchors on the alumina pores. Hernandez et al. [16] have been reported very smooth PPy nanowires by coating the AAM walls with SiO_2 prior to the PPy deposition. They concluded that anionic sites on SiO_2 provide preferential nucleation for PPy along the pore walls. With this study, a relationship between the nanowire dimensions and PEC performances without using any co-surface providers was demonstrated.

In order to form OIH structure, PPy nanowires have been electrochemically deposited on CdS nanowires. For this process, AMM templates with CdS nanowires have been used as working electrode and PPy formation was carried out by cyclic voltammetry. The cross sectional

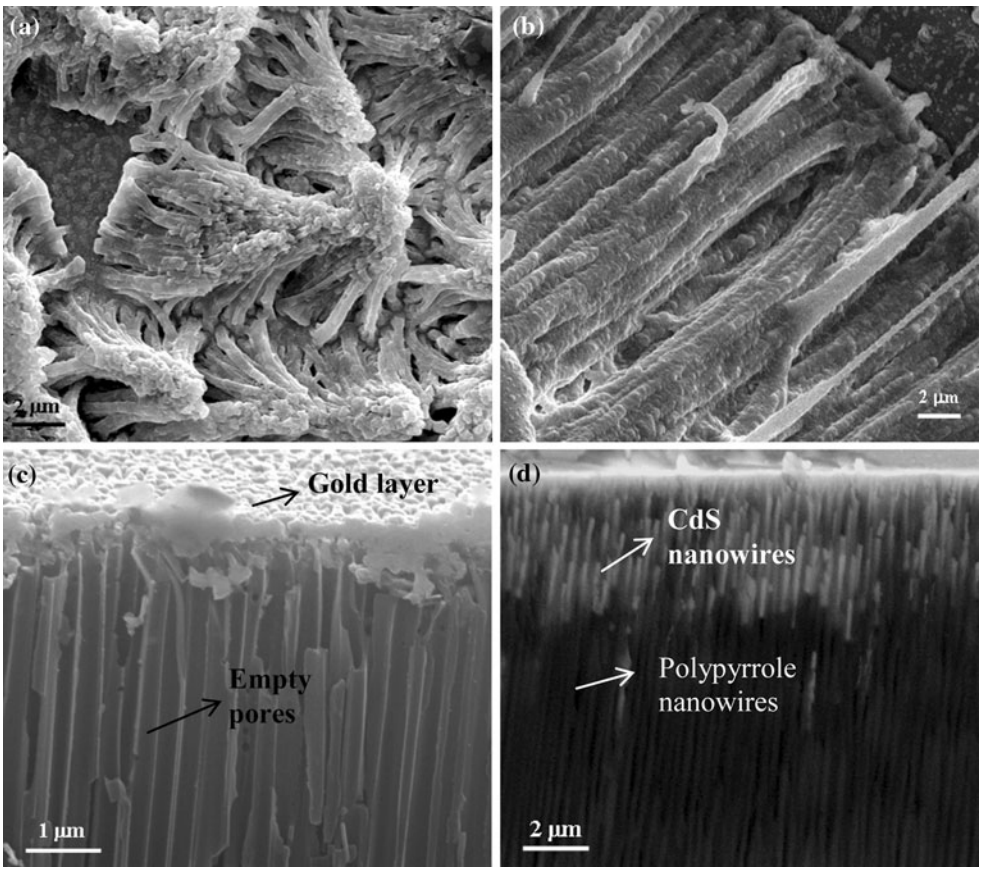

Fig. 4 SEM images of **a** PPy nanowires deposited from 200 scans, **b** PPy nanowires deposited from 800 scans, **c** cross section of gold-coated empty AAM, **d** cross section of AAM after CdS/PPy deposition

SEM images of the gold-coated empty AAM and successfully deposited CdS/PPy nanowires can be seen in Fig. 4c, d.

Structural and optical properties of the CdS and PPy nanowires

XRD analysis (Fig. 5) showed that the characteristic peak of CdS was observed at around 26° (2θ) and 47° (2θ) for all CdS nanowire samples. These peaks can be attributed to (002) hexagonal or (111) cubic [3, 17]. Other minor peaks were most probably due to the gold electrode layer and AAM template itself. Therefore, it can be concluded that CdS nanowires are a mixture of two crystallographic phases: a hexagonal phase (wurtzite) and a cubic phase (zinc blend). Figure 5 also shows that XRD patterns of CdS nanowires synthesized at 30 V are sharper than that of 20 V. This was definitely indicated that the crystal structure was increased with increasing the deposition voltage. EDX analysis showed that nanowires composed of Cd and S (Fig. 6). Moreover, there has been an increase in both Cd and S atomic ratios with increasing the deposition voltage. This supports the observation in SEM analysis where more material deposition was occurred at higher deposition voltages. The optical band gap energy (E_g) was calculated from the following variation of the absorption coefficient (α) with photon energy

$$(\alpha hv) = A(hv - E_g)^n \quad (1)$$

where A is a constant, and n is the power exponent ($n = 1/2$ and $n = 2$ for direct and indirect allowed transitions, respectively). As seen in Fig. 7, $(\alpha hv)^2$ versus photon energy hv with $n = 1/2$ have very good linearity for all samples. This briefly indicates that the optical transition in CdS nanowires is directly allowed. The extrapolation of the straight line of $(\alpha hv)^2$ versus photon energy allows us to obtain the band gap energy values. It has been obtained that there was a minor change in E_g of CdS nanowires, ranging between 2.48 and 2.40 eV, with deposition voltage. As can be seen in Fig. 7, E_g value increased slightly with decreasing the deposition voltage. For different deposition time and temperatures similar results have been obtained.

The chemical structure of the PPy nanowires has been investigated through FTIR analysis. In order to obtain template free nanowires, one side of the AAM has been covered by epoxy and template has been dissolved in 1 M

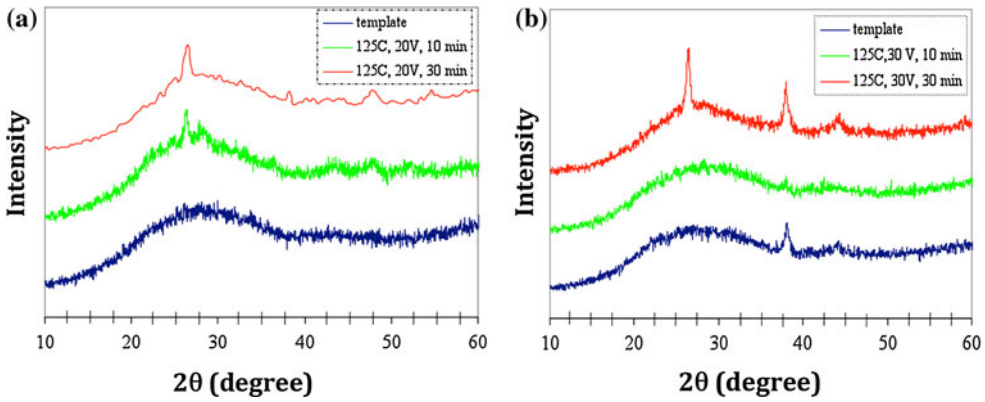

Fig. 5 XRD patterns of CdS nanowires deposited at **a** 20 V and **b** 30 V

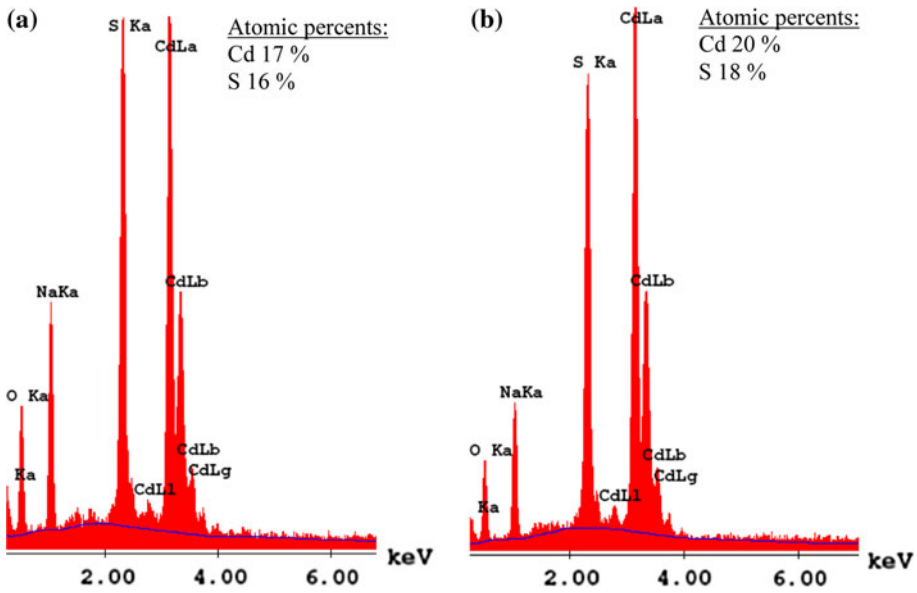

Fig. 6 EDX results of CdS nanowires formed at **a** 125 °C, 20 V, 30 min, **b** 125 °C, 30 V, 30 min

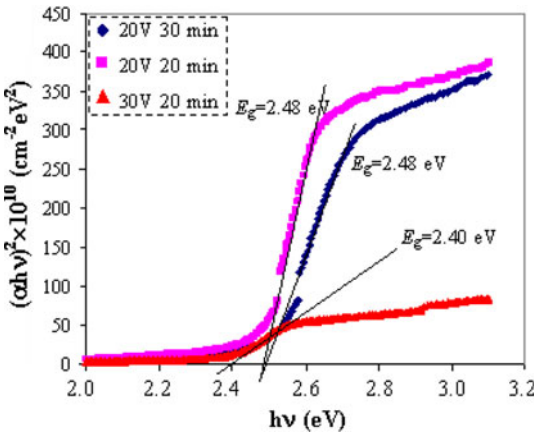

Fig. 7 $(\alpha h\nu)^2$ versus photon energy $h\nu$ plot of CdS nanowires

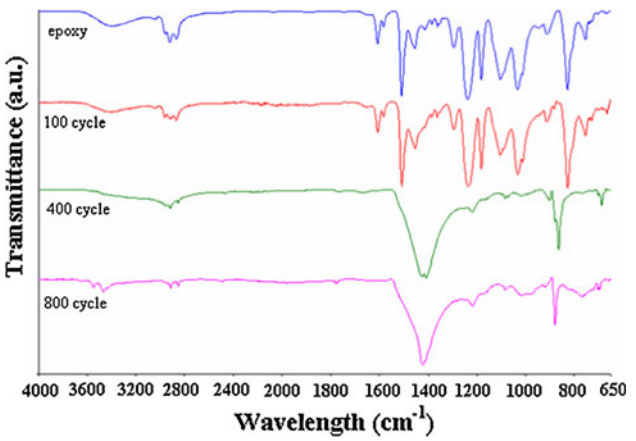

Fig. 8 FTIR spectra of PPy nanowires and blank epoxy

NaOH solution. Then, samples have been dried at 60 °C under vacuum for over night. Figure 8 shows the FTIR spectra of blank epoxy and PPy nanowires deposited for different CV scans. Characteristic absorption bands of the PPy ring structure including the combination of C=C stretch, C–N stretch, and the deformation of the five-membered ring containing the C=C–N, C=C–C groups were observed around 1410 cm^{-1} for the samples deposited for 400 and 800 CV scans [18, 19]. This peak could be

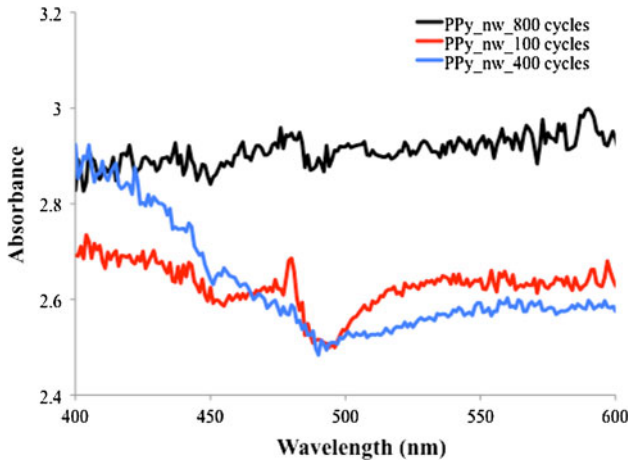

Fig. 9 UV–Vis spectra of PPy nanowires

attributed to typical PPy ring vibration band, which was interestingly demonstrating the wide discrimination of epoxy and PPy nanowire attached on the epoxy. Moreover, the peak shift around the 900 cm^{-1} could be attributed to the =C–H out of plane vibration, indicating polymerization of pyrrole [20]. Although, this polymerization peak at around 900 cm^{-1} was also appeared for the PPy nanowires deposited after lower scans (100 CV scans), peaks from epoxy was dominant at FTIR spectra of this sample. This was most probably due to the less nanowire deposition occurred at 100 CV scan compare to 400 and 800 CV scan.

Chemical structure analysis of PPy nanowires was further investigated by UV–Vis spectrophotometer (Fig. 9). It is known that a fully doped PPy film has two main absorption bands at 886 nm (1.40 eV) and 478 nm (2.60 eV) [21]. The peak around 886 nm associated with the transition between bonding and antibonding polaron levels, whereas the peak around 478 nm corresponded to the transitions from valance band to the anti-bonding polaron state [22]. Depending on the doping level of PPy absorption peaks can shift. Also, the ratio of the absorbance bands at 886 and 478 nm ($\gamma = I_{886}/I_{478}$) indicates the doping level of the polymer: the higher the ratio γ the lower the doping of the polymer [23]. Therefore, the absorption band observed in this study around 480 nm could be attributed to π–π^* transitions in the polymer backbone. The differences in the absorption peaks depending on the number of CV scan could be attributed to the different doping levels. Similar absorption peaks have been previously reported for PPy nanocomposites and nanowires [24–26].

PEC performance of CdS and CdS/PPy nanowires

A PEC cell enables the conversion of the solar energy into chemical energy, which can then be used as fuel. Basically, in a PEC cell with *n*-type semiconductor electrode, a photon having an energy which is equal or greater than the bandgap excites the electrons from valance band to the conduction band. These excited electrons travel through the counter electrode where the reduction of water to form hydrogen gas occurs. Fill factor (FF), which is equal to the ratio of the theoretical power to the actual power of the cell, and the power conversion efficiency (η), a measure of how much of solar energy converted to the electrical energy, are the two key parameters determining the performance of a PEC cell. In this study, both CdS nanowires and CdS/PPy OIH nanowire structures have been used as semiconductor electrode for PEC cell. We have calculated the FF using the following very well-known equation [27]

$$\mathrm{FF}(\%) = \frac{I_{\max} V_{\max}}{I_{\mathrm{sc}} V_{\mathrm{oc}}} \times 100 \tag{2}$$

where $I_{\max}$ and $V_{\max}$ is the maximum current and the voltage, respectively, I_{sc} is the short circuit current, and V_{oc} is the open circuit potential. On the other hand, power conversion efficiency (η) can be calculated from

$$\eta\ (\%\ ) = \frac{I_{\max} V_{\max}}{P_{\mathrm{i}} A} \times 100 \tag{3}$$

where, P_{i} is the power of incident light and A is the area of the electrode. Figure 10 shows a set of linear sweep voltagrams recorded on CdS and CdS/PPy nanowires. For CdS nanowires, the various deposition voltage and time have been chosen to determine the effect of deposition conditions on PEC performances. As can be seen in Fig. 10a, CdS nanowires deposited at 30 V has much higher I_{sc} compare to that of nanowires deposited at 20 V. This result is consistent with SEM, UV–Vis, and X-ray analyses. These analyses showed that 30 V deposition voltage resulted more homogenous and well-distributed nanowires with better crystalline structure compare to the 20 V. Figure 10a also shows that V_{oc} of the CdS deposited at 30 V for 10 min is approximately thrice higher than that of nanowires deposited at 30 V for 30 min. Basically, the open circuit potential for nanowire cell depends on the photocurrent density across the junction area and can be written as [27, 28]

$$V_{\mathrm{oc}} = \left(\frac{kT}{q}\right) \ln\left(\frac{J_{\mathrm{sc}}}{\gamma J_0}\right) \tag{4}$$

where k is the Boltzmann's constant, T the temperature, q the elementary charge, J_{o} the reverse saturation current density over the actual junction area, J_{sc} the short-circuit current density per unit of projected device area, and γ is the ratio of the junction area for a nanowire electrode to a planar electrode, which is given by

$$\gamma = \frac{A_{\mathrm{NW}}}{A_{\mathrm{P}}} = 2\pi r h \rho_{\mathrm{NW}} \tag{5}$$

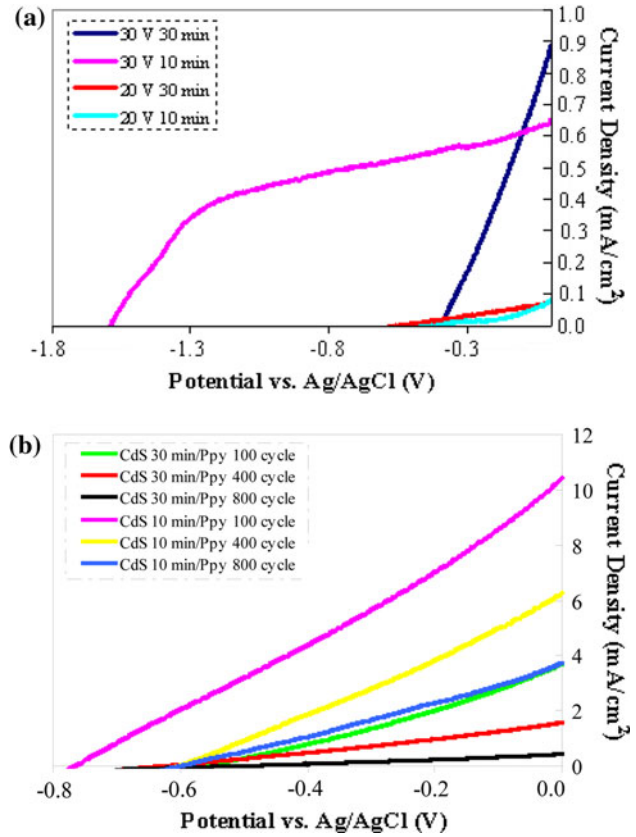

Fig. 10 Potential versus current density graph of **a** CdS nanowires deposited at 125 °C, **b** CdS (deposited at 30 V, 125 °C)/PPy nanowires

where A_{NW} is the junction area of the nanowire array electrode, A_P the area of the planar electrode junction, r the radius of a single nanowire, h the height of the nanowires, and ρ_{NW} is the density of nanowires. Aforementioned, the diameter and the length of the CdS nanowires deposited for 10 min were much smaller than that of nanowires deposited for 30 min. However, the density of nanowires decreased with increasing the deposition time. The average ρ_{NW} for the CdS nanowires deposited at 30 V for 10 and 30 min is approximately 10^9 and 10^7 nanowires/cm^2, respectively. This significant decrease in ρ_{NW} may result the decrease in V_{oc} of the nanowires deposited for 30 min. The highest efficiency of the CdS nanowires obtained in this study is about 1.4% for the nanowires deposited at 30 V for 10 min. Table 1 summarizes all V_{oc}, I_{sc}, FF, and η values for both CdS and CdS/PPy nanowires.

PPy nanowires were deposited on the CdS nanowires formed at optimum voltage of 30 V for 10 and 30 min. As can be seen in Fig. 10b, PEC performances of the CdS nanowires improved significantly after PPy nanowire deposition. As expected, better PEC performances have been observed for the OIH of CdS/PPy nanowires for 10 min CdS deposition. V_{oc} values of the all CdS/PPy heterostructures were comparable and were ranging between 600 and 800 mV. On the other hand, I_{sc} values of the heterostructures changed approximately 24 times by changing the CdS deposition time and number of CV cycle for PPy deposition. The maximum I_{sc} was observed for the 100 CV scans for PPy deposition. This value decreased with increasing the CV scan number. I_{sc} provides information on the net quantum yield for the charge separation and also serves as a measure of the yield of minority carriers that survive the cross of the solid–liquid interface [29]. Like inorganic semiconductors, it is evident that free charges are formed in PPy by photoexcitation [30]. This charge formation can be resulted by the excitation of the mobile charge carriers (charged polarons) either injected at the contacts or created directly via inter-band photoexcitation, or by the lowest energy excitations bound neutral excitons. Therefore, increase in I_{sc} of the PPy nanowires with decreasing the CV scan number can be associated with the more effective excitations of bound neutral excitons. Also, decrease in I_{sc} with increasing the CV scan number may be attributed to the increase in the trap levels in PPy nanowires with more material deposition. As seen in SEM pictures (Fig. 4) surface of the PPy nanowires was

Table 1 V_{oc}, I_{sc}, FF, and η values for the CdS and CdS/PPy nanowires

Material	Condition	V_{oc} (mV)	I_{sc} (mA)	FF (%)	η (%)
CdS nanowire	30 V, 30 min	402	0.89	21.5	0.22
	30 V, 10 min	1590	0.65	45.7	1.36
	20 V, 30 min	562	0.08	23.1	0.03
	20 V, 10 min	418	0.08	15.9	0.02
CdS/PPy nanowire	30 V, 30 min CdS/100 cycle PPy	559	3.70	20.2	1.19
	30 V, 30 min CdS/400 cycle PPy	626	1.57	21.4	0.60
	30 V, 30 min CdS/800 cycle PPy	508	0.44	21.5	0.14
	30 V, 10 min CdS/100 cycle PPy	764	10.5	21.9	5.00
	30 V, 10 min CdS/400 cycle PPy	592	6.25	22.6	2.39
	30 V, 10 min CdS/800 cycle PPy	588	3.72	22.9	1.43

rough, probably indicating that nanowire formation occurs by random nucleation of PPy nanoclusters. Hence, the optical path increases with increasing the nanowire length, which could result the decrease in I_{sc}. The maximum η obtained in this study is about 5.0% for the CdS/PPy heterojunctions, where CdS nanowires were deposited at 30 and 10 min and PPy nanowires were deposited for 100 CV scans. This is one of the highest efficiencies reported in the literature for the nanowire array PEC cells [31, 32]. DC and AC electrical measurements of CdS/PPy hetero nanowires are part of ongoing research.

Chemical stability under dark and illumination are among the key factors affecting the performance of a PEC cell. It has been known that most non-oxide semiconductors such as Si, GaAs, and CdS are not chemically stable in electrolyte solutions. They are in general either dissolved or an oxide layer forms at the semiconductor–electrolyte interface. However, they have very suitable band edge positions to enable reduction/oxidation of water. Therefore, it is very important to improve their resistance against photo-corrosion. Figure 11 indicates the change in I_{sc} with time. For both CdS and CdS/PPy nanowires, I_{sc} stabilized after a certain time, approximately 100 s. These equilibrium currents have been used in FF and η calculations. It is also worth to mention here that the decrease in initial I_{sc} for CdS/PPy nanowires was much smaller compare to that of CdS nanowires. Hence, it is possible to conclude that stability of CdS/PPy hetereojunction nanowires was superior to that of CdS nanowires.

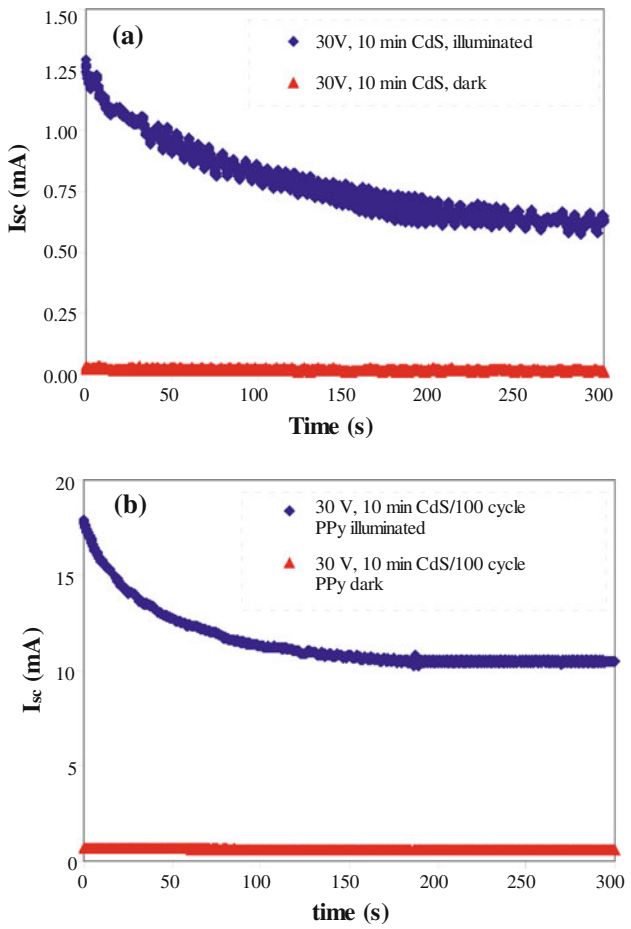

Fig. 11 I_{sc} versus time graphs for **a** CdS nanowires, **b** CdS/PPy nanowires

Conclusions

In this study, CdS and CdS/PPy nanowires have been synthesized using a template-based electrochemical technique. It has been observed that the length and the diameter of the CdS nanowires depend on the deposition time and voltage. The average length and the diameter of the CdS nanowires increased with increasing the deposition time at 30 V. It was demonstrated that both the length and the diameter of the PPy nanowires increased with increasing the CV scan number. XRD analysis showed that CdS nanowires have a peak around 26° (2θ). This peak became more significant by increasing the deposition voltage, indicating the improvement in the crystallinity of the nanowires. UV–Vis showed that there was a minor change in E_g of CdS nanowires, ranging between 2.48 and 2.40 eV, with deposition voltage. UV–Vis and FTIR spectra of the PPy nanowires confirmed that our samples showed typical absorptions peaks of bulk PPy. These absorption peaks can be assigned to π–π^* transitions in the polymer backbone. The maximum η of the CdS nanowires was 1.36%. This efficiency was obtained for the 125 °C, 30 V, and 10 min deposition conditions. On the other hand, efficiencies of the CdS/PPy nanowires were much higher compare to the CdS nanowires. The maximum η obtained in this study was 5.00%, indicating that heterojunctions of CdS nanowires with PPy nanowires have a great potential to use in PEC cell applications.

Acknowledgement This study was supported by The Scientific and Technological Research Council of Turkey under the research Grant TBAG-107T354.

References

1. Mansur HS, Vasconcelos WL, Grieser F, Caruso F (1999) J Mater Sci 34:5285. doi:10.1023/A:1004784501939
2. Jia H, Xu H, Hu Y, Tang Y, Zhang L (2007) Electrochem Commun 9:354
3. Dongre JK, Nogriya V, Ramrakhiani M (2009) Appl Surf Sci 255:6115
4. Jang JS, Joshi UA, Lee JS (2007) J Phys Chem C 111:13280
5. Bredol M, Matras K, Szatkowski A, Sanetra J, Prodi-Schwab A (2009) Sol Energ Mater Sol Cell 93:662
6. Chanyawadee S, Lagoudakis PG, Harley RT, Lidzey DG, Henini M (2008) Phys Rev B 77:193402/1

7. Pasquier AD, Mastrogiovanni DDT, Klein LA, Wang T, Garfunkel E (2007) Appl Phys Lett 91:183501/1
8. Gonchera G, Noice L, Solanki R (2008) J Exp Nanosci 3:77
9. Thitima R, Patcharee C, Takashi S, Susumu Y (2009) Solid State Electron 53:176
10. Lei Z, Wei X, Zhang L, Bi S (2008) Colloid Surf A 324:131
11. Jiang L, Fu Y, Li H, Hu W (2008) J Am Chem Soc 130(12):3937
12. Chiu BJ-J, Kei C-C, Perng T-P, Wang W-S (2003) Adv Mater 15:1361
13. Dong H, Jiang S, Jiang L, Liu Y, Li H, Hu W, Wang E, Yan S, Wei Z, Xu W, Gong X (2009) J Am Chem Soc 131(47):17315
14. Mondal SP, Dhar A, Ray SK (2007) Mater Sci Semicon Process 10:185
15. Reynes O, Demoustier-Champagnez S (2005) J Electrochem Soc 152:D130
16. Hernandez SC, Chaudhuri D, Chen W, Myung NV, Mulchandani A (2007) Electroanal 19:2125
17. Li Y, Huang F, Zhang Q, Gu Z (2000) J Mater Sci 35:5933. doi:10.1023/A:1026714004563
18. Wan X, Zhang W, Jin S, Xue G, You Q-D, Che B (1999) J Electroanal Chem 470:23
19. Ma X, Li G, Wang M, Chen H (2006) J Mater Sci 41:7604. doi:10.1007/s10853-006-0849-2
20. Vishnuvardhan TK, Kulkarni VR, Basavaraja C, Raghavendra SC (2006) Bull Mater Sci 29:77
21. Geetha S, Trivedi DC (2004) Mater Chem Phys 88:388
22. Alfaro-Lopez HM, Aguilar-Hernandez JR, Garcia-Borquez A, Hernandez-Perez MA, Contreras-Puente GS (2009) Interface Controlled Org Thin Films 129:73
23. Lewis T, Wallace G, Kim C, Kim D (1997) Synth Met 84–86:403
24. Karim MR, Yeum JH (2008) J Polym Sci Pol Phys 46:2279
25. Koo YK, Kim BH, Park DH, Joo J (2004) Mol Cryst Liq Cryst 425:55[333]
26. Joo J, Park KT, Kim BH, Kim MS, Lee SY, Jeong CK, Lee JK, Park DH, Yi WK, Lee SH, Ryu KS (2003) Synth Met 135–136:7
27. Würfel P (2005) Physics of solar cells, from principles to new concepts. Wiley-VCH, Berlin
28. Tetsuo S (2006) Nanostructured materials for solar energy conversion. Elsevier, Amsterdam
29. Lewis NS (1990) Acc Chem Res 23:176
30. Kilmartin PA, Wright GA (2001) Electrochim Acta 46:2787
31. Yang X, Wolcott A, Wang G, Sobo A, Fitzmorris RC, Qian F, Zhang JZ, Li Y (2009) Nano Lett 9:2331
32. Shim HS, Shinde VR, Kim JW, Gujar TP, Joo OS, Kim HJ, Kim WB (2009) Chem Mater 21:1875